

Graph Edit Distance Learning via Different Attention

Jiaxi Lv¹ Liang Zhang² Yi Huang¹ Jiancheng Huang¹ Shifeng Chen^{1*}

¹Shenzhen Institute of Advanced Technology

²Xidian University

jx.lv1@siat.ac.cn

Abstract

Recently, more and more research has focused on using Graph Neural Networks (GNN) to solve the Graph Similarity Computation problem (GSC), i.e., computing the Graph Edit Distance (GED) between two graphs. These methods treat GSC as an end-to-end learnable task, and the core of their architecture is the feature fusion modules to interact with the features of two graphs. Existing methods consider that *graph-level* embedding is difficult to capture the differences in local small structures between two graphs, and thus perform fine-grained feature fusion on *node-level* embedding to improve the accuracy, but leads to greater time and memory consumption in the training and inference phases. However, this paper proposes a novel *graph-level* fusion module **Different Attention (DiffAtt)**, and demonstrates that graph-level fusion embeddings can substantially outperform these complex node-level fusion embeddings. We posit that the relative difference structure of the two graphs plays a key role in calculating their GED values. To this end, DiffAtt uses the difference between two graph-level embeddings as an attentional mechanism to capture the graph structural difference of the two graphs. Based on DiffAtt, a new GSC method, named **Graph Edit Distance Learning via Different Attention (REDRAFT)**, is proposed, and experimental results demonstrate that **REDRAFT achieves state-of-the-art performance in 23 out of 25 metrics in five benchmark datasets**. Especially on MSE, it respectively outperforms the second best by 19.9%, 48.8%, 29.1%, 31.6%, and 2.2%. Moreover, we propose a quantitative test **Remaining Subgraph Alignment Test (RESAT)** to verify that among all *graph-level* fusion modules, the fusion embedding generated by DiffAtt can best capture the structural differences between two graphs.

1 Introduction

Graph similarity computation (GSC) is a fundamental problem for graph-based applications, e.g., drug design (Tian et al. 2007), graph similarity search (Zeng et al. 2009; Liang and Zhao 2017), and graph clustering (Wang et al. 2020). **Graph Edit Distance (GED)**, which is defined as the least number of graph edit operators to transform graph G_i to graph G_j , is one of the most popular graph similarity metrics (Gao et al. 2010; Neuhaus, Riesen, and Bunke 2006; Bougleux et al. 2015). Unfortunately, the exact GED computation is NP-Hard in general (Zeng et al. 2009), which is

too expensive to leverage in practice.

Recently, many Graph Neural Networks (GNNs) based GSC methods have been proposed to compute the GED in a faster manner (Bai et al. 2019a, 2020; Li et al. 2019; Ling et al. 2021; Qin et al. 2021; Zhang et al. 2021; Bai and Zhao 2021; Wang et al. 2021; Ranjan et al. 2022; Zhuo and Tan 2022). The GNN-based algorithms transform the GED value to a similarity score and use an end-to-end framework to learn to map the given two graphs to their similarity score. As a general framework, the Siamese neural network is used to aggregate information on each graph, while the feature fusion module is used to capture the graphs’ similarity representation, and then the Multi-layer Perceptron (MLP) is leveraged for the similarity score regression.

As discussed by Qin et al., capturing the interaction between two graphs is instrumental in tackling the GSC problem. Thoroughly modeling the intricate interplay between graphs is crucial for accurately characterizing their similarity. Most of the existing GSC methods drop the graph-level fusion module and instead interact on node-level embeddings to learn the similarities between two graphs in a more fine-grained way, i.e., computing the similarity or attention between all nodes of two graphs (Li et al. 2019; Bai et al. 2020; Ling et al. 2021). It is believed that the differences between one graph and other graphs may be on any small local structure, but the graph-level embedding of each graph is a fixed one vector and it is difficult to reflect these small differences information flexibly (Bai et al. 2020). *However, node-level fusion entails computational and memory costs that scale quadratically with the number of nodes, presenting challenges for large-scale graphs.* To address these issues, the Alignment Regularization (AReg) (Zhuo and Tan 2022) imposes constraints on the GNN Encoder during training to enable it to learn representations that capture the underlying alignment between nodes across a pair of graphs. This helps the model learn cross-graph interactions in graph-level embeddings without needing to explicitly compute node-to-node similarities. *However, the regularization strength hyperparameter λ of AReg needs proper tuning to prevent the regularization term from adversely affecting the model.*

Developing graph-level fusion modules tailored for GSC still remains an open challenge. Many existing designs like Neural Tensor Networks (NTN) (Socher et al. 2013) or Embedding Fusion Network (EFN) (Qin et al. 2021) are largely

*Corresponding author

based on intuition rather than principled analysis. However, we find in Sec 3 that *the GED is only correlated with the discrepancy in the two graph structures and thus concludes that the graph-level fusion module should capture the structural differences between two graphs*. Inspired by this, we propose a novel graph-level fusion module **DiffAtt**. Especially, DiffAtt generates an attention vector reflecting the relative structural differences between two graphs, and this attention is leveraged to update each graph-level representation via element-wise multiplication, resulting in new representations encoding the structural differences. Moreover, we propose a novel GSC architecture that outperforms existing node-level fusion models and achieves state-of-the-art performance. To sum up, the contributions of this paper can be summarized as follows:

1. A novel graph-level fusion module, **DiffAtt** is proposed, which is an attention mechanism to highlight structural differences between two graphs. Experimental results demonstrate that DiffAtt has strong generalization and can substantially improve the performance of the model.
2. Based on DiffAtt, a GSC model, **Graph Edit Distance Learning via Different Attention (REDRAFT)** is proposed. In addition to the DiffAtt, REDRAFT uses multi-scale GIN layers to extract more representative graph-level embeddings, each of which contains residual connections and an additional Forward Forward Network (FFN) to enhance node features. Compared with current methods on five benchmark datasets, REDRAFT achieves state-of-the-art performance on 23 out of 25 metrics.
3. To verify the ability to extract graph structural difference information, a quantitative test **Remaining Sub-graph Alignment Test (RESAT)** is proposed, and the results demonstrate that the ability of the graph-level fusion module to extract graph structural difference information is positively correlated with the performance on GSC, while **DiffAtt** has the strongest ability to extract graph structural difference information.

2 Preliminary and Related Work

In this section, we introduce the notations, the definitions of GED and GSC, and the related works.

Notations. The graph data G can be viewed as a pair of the set of nodes $V = \{v_i\}_{i=1}^N$ and the set of edges E . The $|V| = N$ represents the number of nodes. In our setting, all graphs are undirected and edges have no attributes. Therefore, the structure of the graph can be represented using the adjacency matrix $A \in \{0, 1\}^{N \times N}$ and the nodes v_i and v_j are connected by an edge if and only if $A_{i,j} = 1$. The node feature matrix is $X \in \mathbb{R}^{N \times C}$. C is the dimension of its features. $x_i = \xi(v_i)$, where $\xi(\cdot)$ maps node v_i to node feature $x_i \in \mathbb{R}^C$.

Graph Edit Distance (GED). The graph edit distance (GED) is a measure of the minimum *dissimilarity* between two graphs G_1 and G_2 , which is defined as the minimum cost of transforming G_1 to become isomorphic with G_2 . Specifically, a graph edit operator e_i can be a node or edge insertion, removal, or substitution. An edit path $\mathcal{P}(G_1, G_2)$

is a sequence of graph edit operators that transform G_1 into a graph isomorphic to G_2 . The graph edit distance (GED) is defined as:

$$GED(G_1, G_2) = \min_{\{e_1, e_2, \dots, e_k\} \in \mathcal{P}(G_1, G_2)} \sum_{i=1}^k c(e_i) \quad (1)$$

where $c(e_i)$ denotes the real non-negative cost function of the i -th edit operator e_i in the edit sequence $\{e_1, e_2, \dots, e_k\}$. We follow the setting of prior work (Bai et al. 2019a), defining all $c_e(\cdot)$ as 1.

Graph Similarity Computation Problem (GSC). GED can effectively capture the edge and node differences between two graphs and has been widely used in real-world scenarios (Bai et al. 2019a; Zhuo and Tan 2022). Therefore, the GSC adopts GED as the ground truth similarity value. In order to better conform to the learning paradigm of GNNs, the GED is normalized as $nGED(G_i, G_j) = \frac{GED(G_i, G_j)}{(|N_i| + |N_j|)/2}$, and the similarity score between two graphs is defined as $s(G_i, G_j) = \exp(-nGED(G_i, G_j))$, which is in the range of $(0, 1]$. The GSC is defined as: given two graphs G_i and G_j with their similarity metric, the GSC models learn a function that maps the two graphs to their similarity score $s(G_i, G_j)$.

Related Work. The Graph Matching Network (GMN) proposed by Li et al. is the first GNN-based GSC model. It computes similarity via cross-graph node-to-node attention mechanisms. Bai et al. proposed the SimGNN model, which uses GCN layers (Kipf and Welling 2016) to update node embeddings and uses the Neural Tensor Networks (NTN) (Socher et al. 2013) module to learn graph fusion embeddings in the two graph-level embeddings. However, their later work (Bai et al. 2020) argued that the small local structural differences are difficult to be captured by a single graph embedding vector, and thus proposed GraphSim, which directly learns the similarity based on the node-level interaction of the two given graphs. Motivated by this, H2MN (Zhang et al. 2021) designed a hierarchical node-level interaction module, while MGMN (Ling et al. 2021) proposed a more complex node-graph level interaction module. Many recent works have focused on designing complex, fine-grained fusion modules, under the belief that modeling node-level interactions is key for accuracy. However, relying on the complex node-level fusion entails significant costs in memory, training time, and inference speed due to the quadratic growth in computational complexity. To address this, Zhuo and Tan proposed the Alignment Regularization technique that enables graph-level embeddings to better capture cross-graph interactions without needing expensive node-level fusion. By regularizing the GNN Encoder during training, their method aligns the graph embeddings to remove the need for direct node-level feature comparisons, demonstrating that this graph-level approach can achieve competitive or better performance compared to node-level fusion.

Our work presented the same conclusion as Zhuo and Tan, showing that feature fusion on graph-level embeddings can also lead node-level or node-graph-level fusion embeddings substantially. However, the difference of REDRAFT from the previous approaches is: 1). REDRAFT uses a new graph-

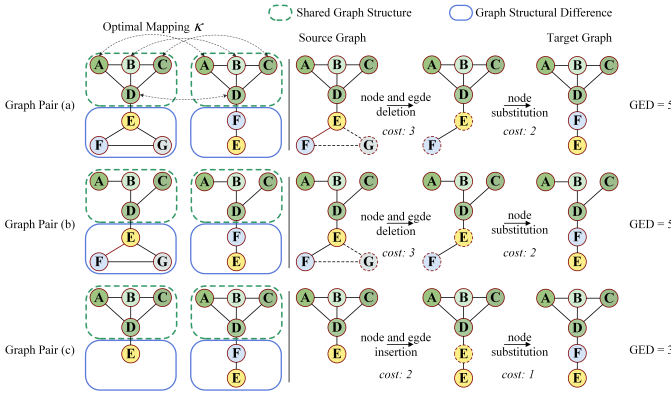


Figure 1: Graph edit processes for some graph pairs.

level fusion module DiffAtt to better explore the differences between the two graph structures; 2). REDRAFT uses *residual connections* to help optimize the model training process, and adds the *FFN* to augment the nonlinear transformations to learn a more discriminative representation of the graph-level embeddings.

3 Motivation

Compared to other graph learning tasks, the GSC model needs to effectively fuse the features of two graphs to learn their similarity. However, there has been little principled analysis on what role a graph fusion module should fulfill to enable accurate GED computation. In this section, we analyze the GED and graph matching problem, derive the key responsibilities of the graph-level fusion module, and discuss the existing graph-level fusion modules.

GED is a form of graph matching problem. Graph matching aims to find an optimal mapping that maximizes the similarity between two graphs. However, GED as a measure of the minimum difference between two graphs, focuses more on the structural difference between two graphs under their optimal mapping. Assume that the optimal bijective mapping between two graphs G_1 and G_2 is $\kappa: \hat{V}_1 \rightarrow \hat{V}_2$ between $\hat{V}_1 \subseteq V_1$ and $\hat{V}_2 \subseteq V_2$ such that node features are preserved, i.e., $\xi(v) = \xi(\kappa(v))$. Specifically, we define two edge sets $\hat{E}_1 \subseteq E_1$ and $\hat{E}_2 \subseteq E_2$ that satisfy if $(u, v) \in \hat{E}_1$, where $u, v \in \hat{V}_1$, these must exist $(\kappa(u), \kappa(v)) \in \hat{E}_2$. The optimal mapping between two graphs divides the two graphs into two separate components, respectively:

1. The **shared graph structure** component, represented by (\hat{V}_1, \hat{E}_1) , containing the substructures that is common between both graphs.
2. The **graph structural difference** component, e.g., $(V_1 - \hat{V}_1, E_1 - \hat{E}_1)$ for G_1 , containing substructure that one graph holds and the other does not.

We observe that graph editing operations are not performed on the shared graph structure. Therefore, we can derive a key insight into the role of shared graph structure versus graph structural difference in determining GED values:

Observation 1. *Under the optimal mapping, the GED is solely determined by the graph structural difference of the two graphs, and their shared graph structure have no impact on their GED value.*

Fig 1 shows the impact of shared graph structure and graph structural difference between several graph pairs on the GED values. Although graph pairs (a) and (b) have different shared graph structure parts, they have the same graph structural difference parts and thus the same optimal edit path and GED value. In contrast, graph pairs (a) and (c) have the same shared graph structure parts, but different graph structural difference parts, leading to different optimal edit paths and GED values. Based on this insight, we hypothesize that the fusion module can enable more accurate GED modeling by focusing on capturing graph structural difference rather than shared graph structure.

However, most graph-level fusion modules do not directly aim to extract graph structural difference. A widely used learnable graph-level fusion module is the Neural Tensor Networks (NTN) module (Socher et al. 2013; Bai et al. 2019a; Zhuo and Tan 2022), which is defined as:

$$NTN(\mathbf{h}_i, \mathbf{h}_j) = f(\mathbf{h}_i^T W^{[1:K]} \mathbf{h}_j + V[\mathbf{h}_i, \mathbf{h}_j] + b), \quad (2)$$

where \mathbf{h}_i and \mathbf{h}_j denote the embeddings of graph G_i and G_j , respectively. $W^{[1:K]} \in \mathbb{R}^{C \times C \times K}$, $V \in \mathbb{R}^{K \times 2C}$ and $b \in \mathbb{R}^K$ are the learnable parameters. The advantage of the NTN module lies in allowing the interaction between two graph-level features through multiplication in the first term (Socher et al. 2013). However, if the learnable parameter $W^{[1:K]}$ is assumed to be an identity matrix, the first term of NTN can degenerate into the inner product of two graph embeddings, which indicates that **NTN may prefer to compute similarities rather than differences between two graphs**. The Embedding Fusion Network (EFN) is another graph-level fusion module, which is defined as $EFN(\mathbf{h}_{ij}) = MLP(\sigma(W_U \delta(W_D \mathbf{h}_{ij})) \cdot \mathbf{h}_{ij} + \mathbf{h}_{ij})$, where \mathbf{h}_{ij} denotes the concatenation of the two graph embeddings. σ and δ denote the sigmoid gating and ReLU function, respectively. Although EFN enhances the fusion representation of two graph embeddings through MLPs, **it does not selectively highlight graph structural difference features**. In addition to NTN and EFN, the element-wise absolute distance or squared distance is another commonly used fusion module, which is defined as $|\mathbf{h}_i - \mathbf{h}_j|^p$, where the order p is respectively set to 1 or 2. While these methods aim to highlight graph structural difference by directly computing the difference between the embeddings, **they perform poorly in practice, likely because subtractive operations discard the rich details within graph structural difference**.

However, this paper proposes a novel graph-level fusion module, named **Different Attention (DiffAtt)**. DiffAtt leverages the difference between the two embeddings as a form of attention to highlight graph structural difference features in graph-level embeddings, which allows for more graph structural difference detailed features to be retained. We find that DiffAtt can substantially improve performance, outperforming even complex node-level fusion models. Furthermore, as validated quantitatively in Sec 6, DiffAtt ap-

pears to capture detail graph structural difference information better than other graph-level fusion methods and therefore can better improve the performance of the model.

4 Proposed Methods

In this section, we first introduce the *DiffAtt* and then present the overall architecture of the *Graph Edit Distance Learning via Different Attention (REDRAFT)* model.

4.1 Different Attention (DiffAtt)

As motivated in Sec 3, DiffAtt aims to highlight the relatively graph structural difference of the two graphs. Although directly using the distance between two embeddings can encode differences, it may lose fine-grained details about graph structural differences. Since rich graph structural difference features are already contained in the graph-level embeddings, DiffAtt uses the discrepancy between the graph-level embeddings to guide an attention mechanism that amplifies graph structural difference features, while suppressing shared graph structure features.

First, we take the two graph embeddings \mathbf{h}_i and \mathbf{h}_j and calculate the element-wise absolute difference between them. This gives us a new representation that encodes the variation between the graph embeddings. *Second*, we pass this through a MLP to adjust and refine the difference information as $\mathbf{h}_{diff} = MLP(|\mathbf{h}_i - \mathbf{h}_j|)$. *Next*, a softmax function converts these differences into attention weights as $\alpha = softmax(\mathbf{h}_{diff} \cdot t^{-1})$, with higher values indicating dimensions that diverge more across the graphs, and t is the temperature factor to control the smoothness of the difference. *Finally*, we multiply α element-wise with the original graph embeddings as $\mathbf{u}_{G_i} = \alpha \odot \mathbf{h}_i$ and $\mathbf{u}_{G_j} = \alpha \odot \mathbf{h}_j$. This selectively amplifies the dimensions of graph structural difference, while suppressing aspects of shared graph structure.

4.2 Architecture of REDRAFT

Based on the DiffAtt, we propose a new GSC model named Graph Edit Distance Learning via Different Attention (REDRAFT). The architecture of REDRAFT is $f(G_i, G_j) = \Theta(F(E(G_1), E(G_2)))$, where $E(\cdot)$ is a GNN Encoder that generates more representative embeddings for each graph independently, $F(\cdot, \cdot)$ is a graph-level fusion module, implemented as our proposed DiffAtt, and $\Theta(\cdot)$ is an MLP regressor that maps the fused embedding generated by F to the similarity score. Fig 2 shows the block diagram of the REDRAFT and the details are as follows:

In order to better leverage DiffAtt, we believe that our GNN Encoder should satisfy two properties. The first one is the need to satisfy the *permutation invariance* to implicitly align two graphs. Finding the optimal mapping between two graphs is equivalent to permuting nodes to match across graphs. By making the GNN Encoder permutation invariant, it can implicitly align the two input graphs when encoding them using shared parameters. This allows DiffAtt to better focus on modeling the graph structural difference between the aligned graphs. The second one is having *strong expressive power* to extract graph detail information in graph-level

embeddings, which can help DiffAtt better capture the information of graph structural difference.

The Graph Isomorphism Network (GIN) (Xu et al. 2018) has the same expressive power as the Weisfeiler-Lehman (WL) graph isomorphism test, i.e. determining whether two graphs are non-isomorphic. Therefore, we choose GIN as our GNN layer to update the embedding of the nodes, which is defined as:

$$GIN(x_i^{(k)}) = MLPs \left((1 + \epsilon) \cdot x_i^{(k)} + \sum_{j \in \mathcal{N}(i)} x_j^{(k)} \right), \quad (3)$$

where ϵ is a learnable parameter or a fixed scalar and k stands for at the k^{th} layer. $\mathcal{N}(i)$ denotes the neighbors of node i . All the MLPs in GIN have one linear layer with the Layer Normalization (Ba, Kiros, and Hinton 2016) and ReLU activation function. *To promote model training optimization and boost the expressiveness of node embeddings, we enhance GIN layers with Residual Connections (He et al. 2016) and FeedForward Neural Network (FFN) as $x_i^{(k+1)} = FFN(x_i^{(k)} + GIN(x_i^{(k)}))$.* Lower layers capture local neighborhood information while higher layers capture more global patterns. Thus, we use K layers of GIN to aggregate information from neighboring nodes in multiple stages, and extract the features X^k from the output of each layer of GIN. The learnable Global Context-Aware Attention (GCA) (Bai et al. 2019a) is leveraged as our graph-level readout function, because it learns the attention of nodes based on global context information to obtain graph-level representations with strong expressive power and discriminativity. GCA is defined as:

$$\begin{aligned} \mathbf{c}^{(k)} &= \tanh\left(\left(\frac{1}{N} \sum_{i=1}^N x_i^{(k)}\right) W^{(k)}\right) \\ \mathbf{h}^{(k)} &= \mathcal{F}_{CBA}(X^{(k)}) = \sum_{i=1}^N \sigma(x_i^{(k)T} \mathbf{c}^{(k)}) x_i^{(k)}, \end{aligned} \quad (4)$$

where $\mathbf{c}^{(k)}$ denotes the context information of the graphs, and $W^{(k)} \in \mathbb{R}^{C^{(k)} \times C^{(k)}}$ is the learnable parameter. *Based on this architecture, our GNN Encoder not only satisfies permutation invariance but also generates more expressive graph-level embeddings.*

DiffAtt is applied to the graph-level embeddings obtained at each layer to generate fused embeddings at multi-scale, and all the enhanced embeddings $\mathbf{u}_{G_i}^{(k)}$ and $\mathbf{u}_{G_j}^{(k)}$ are concatenated to obtain the multi-scale fused embedding as $\mathbf{u}_{G_i, G_j} = \text{concat}([\mathbf{u}_{G_i}^{(0)}, \mathbf{u}_{G_j}^{(0)}, \dots, \mathbf{u}_{G_i}^{(K)}, \mathbf{u}_{G_j}^{(K)}])$. A MLP with two hidden layers and ReLU activation is then applied to map \mathbf{u}_{G_i, G_j} to the similarity score. We do not use a sigmoid output to avoid training instability, and we adopt the **Mean Square Error (MSE)** as the loss function to train REDRAFT.

Time Complexity Analysis. The time complexity of GIN is $\mathcal{O}(\max(E_i, E_j))$ and the time complexity of the FFN, DiffAtt, and MLP regressors are all $\mathcal{O}(C \times C)$. Compared to cross-graph node-level interactions with complexity $\mathcal{O}(N_i \times$

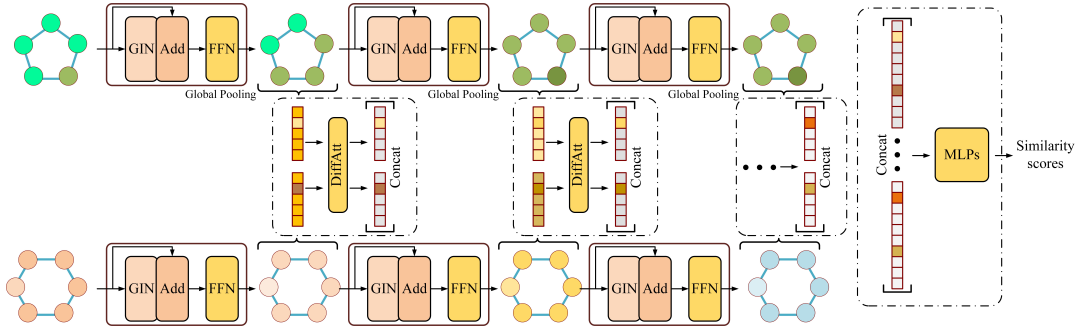


Figure 2: REDRAFT first uses the multi-scale GIN Encoder to aggregate the information in the graph, then DiffAtt for feature fusion, and finally MLP to predict the similarity scores.

N_j), REDRAFT’s DiffAtt has lower complexity and faster inference, especially on large-scale graphs.

5 Experiments

In this section, we evaluate our method using the five benchmark datasets provided by Bai et al. (2019a,b) in GSC and compare our method with other methods.

The **REDRAFT** is evaluated using the PyTorch Geometric (Fey and Lenssen 2019). Following the setup of the previous work, we use the Adam optimizer with a learning rate of 0.001 and batch size set to 128. All hidden channels are set to 64 in REDRAFT. Typically, we run 18 epochs on each dataset and perform 20 validations uniformly on the last epochs. Since the NCI109 dataset is relatively large, we only run 10 epochs. Ultimately, the parameter that results in the least validation loss is chosen to perform the evaluations on the test data. Note that all the experiments are performed on a Linux server with Intel(R) Xeon(R) CPU E5-2690 v4 @ 2.60GHz and 8 NVIDIA GeForce RTX 3090Ti. The experiments are conducted on five widely used graph similarity benchmark datasets: AIDS700nef (Bai et al. 2019a), LINUX (Wang et al. 2012), IMDBMulti (Yanardag and Vishwanathan 2015), PTC (Shrivastava and Li 2014) and NCI109 (Wale, Watson, and Karypis 2008). We evaluate model performance using several common metrics: Mean Square Error (MSE, in the format of 10^{-3}), Spearman’s Rank Correlation Coefficient (ρ) (Spearman 1961), Kendall’s Rank Correlation Coefficient (τ) (Kendall 1938), and Precision at k ($P@k$) (Bai et al. 2019a). Details of the datasets, data processing, evaluation metrics, and other details are included in the Appendix. All code and trained model parameters are available in the supplementary material.

5.1 Ablation Study

In this subsection, we validate the key design choices for our model by evaluating the impact of different components.

Efficiency and Generalization of DiffAtt. To verify the efficiency and generalization of DiffAtt, we evaluated it under four graph-level readout module settings. The four graph-level readout functions are Global Mean Pooling, Global Sum Pooling, Global Max Pooling and GCA. The temperature t of DiffAtt here is set to 1 and the rest of the

Readout	DiffAtt	AIDS700nef		LINUX		IMDBMulti		PTC		NCI109	
		MSE ↓	ρ ↑	MSE ↓	ρ ↑	MSE ↓	ρ ↑	MSE ↓	ρ ↑	MSE ↓	ρ ↑
Mean	✗	3.027	0.812	0.541	0.985	0.495	0.864	5.707	0.746	4.596	0.516
	✓	2.075 [†]	0.864 [†]	0.311 [†]	0.989 [†]	0.343 [†]	0.928 [†]	4.711 [†]	0.791 [†]	4.388 [†]	0.540 [†]
Max	✗	3.225	0.805	0.356	0.989	0.403	0.853	4.385 [†]	0.818	4.030	0.595 [†]
	✓	2.060 [†]	0.855 [†]	0.232 [†]	0.991 [†]	0.311 [†]	0.920 [†]	4.414	0.821 [†]	3.922 [†]	0.584
Sum	✗	1.427	0.901	0.122	0.992	0.387	0.859	1.539	0.944	3.650	0.680
	✓	1.096 [†]	0.921 [†]	0.062 [†]	0.994[†]	0.316 [†]	0.929[†]	1.040 [†]	0.961 [†]	3.587[†]	0.686[†]
GCA	✗	1.389	0.906	0.115	0.992	0.377	0.856	1.655	0.938	3.501 [†]	0.671
	✓	1.076[†]	0.923[†]	0.048[†]	0.994[†]	0.296[†]	0.914 [†]	1.015[†]	0.962[†]	3.727	0.675 [†]

Table 1: Experimental results on the efficiency and generalization of DiffAtt. The [†] represents the best performance with or without DiffAtt, while the bold denotes the best performance of the four graph readout functions. The [†] means that the larger this indicator is, the better the performance, while the [↓] indicates the opposite.

GNN	t	ENH	AIDS700nef		IMDBMulti		PTC	
			MSE ↓	ρ ↑	MSE ↓	ρ ↑	MSE ↓	ρ ↑
GCN	1	✓	1.077	0.921	0.313	0.938 [†]	1.059	0.961
GAT	1	✓	1.147	0.913	0.332	0.901	1.029	0.962[†]
GIN	1	✗	1.238	0.909	0.717	0.930	1.054	0.960
GIN	1	✓	1.076 [†]	0.923 [†]	0.296[†]	0.914	1.015 [†]	0.962[†]
GIN	0.5	✓	1.159	0.919	0.303	0.958	1.056	0.962
GIN	2	✓	1.052	0.923	0.319	0.951	1.029	0.955
GIN	4	✓	1.051	0.923	0.310	0.940	0.995	0.951
GIN	learnable	✓	1.037	0.925	0.299	0.904	0.993	0.962

Table 2: Experimental results on using different GNNs, temperature factor t , and enhancement (ENH). [†] represents the best performance in the first four experiments. The bold denotes the best performance with all configurations.

experimental setup and network architecture are the same as those used in Sec 5.2. We report the MSE and ρ metrics of each dataset in Table 1. Surprisingly, **DiffAtt can effectively boost 37 of the 40 metrics on the five benchmark datasets for the four graph readout functions, which proves that DiffAtt has strong generalization abilities under different settings.** Specifically, on the MSE of the LINUX dataset, DiffAtt brings 43% (0.541 vs. 0.311), 35% (0.356 vs. 0.232), 49% (0.122 vs. 0.062), and 58% (0.115 vs. 0.048) improvement for each of the four graph readout settings, which demonstrates the efficiency of DiffAtt. GCA, due to its ability to dynamically adjust the weight of each node based on the global information, achieves better performance in most of the datasets. However, sum pooling works

	AIDS700nef					LINUX					IMDBMulti					PTC					NCI109				
	MSE ↓	ρ ↑	τ ↑	P@10 ↑	P@20 ↑	MSE ↓	ρ ↑	τ ↑	P@10 ↑	P@20 ↑	MSE ↓	ρ ↑	τ ↑	P@10 ↑	P@20 ↑	MSE ↓	ρ ↑	τ ↑	P@10 ↑	P@20 ↑	MSE ↓	ρ ↑	τ ↑	P@10 ↑	P@20 ↑
GMN	1.294	0.909	0.772	0.604	0.705	0.086	0.994	0.963	0.99	0.984	0.848	0.885	0.793	0.831	0.839	2.134	0.956	0.835	0.570	0.682	3.734	0.655	0.511	0.126	0.125
SimGNN	2.057	0.867	0.716	0.487	0.588	0.922	0.976	0.907	0.942	0.946	0.481	0.918	0.839	0.857	0.874	1.451	0.948	0.821	0.559	0.649	3.650	0.667	0.522	0.104	0.136
EGSC	1.595	0.890	0.746	0.576	0.655	0.580	0.984	0.954	0.969	0.966	0.431	0.906	0.834	0.880	0.889	6.964	0.594	0.454	0.326	0.436	3.841	0.669	0.525	0.145	0.174
ERIC	1.361	0.904	0.765	0.629	0.706	0.147	0.993	0.961	0.989	0.990	0.422	0.891	0.820	0.873	0.873	1.789	0.905	0.753	0.532	0.640	3.833	0.693	0.539	0.150	0.165
GraphSim	1.581	0.894	0.751	0.580	0.675	0.130	0.994	0.966	0.987	0.99	0.515	0.907	0.830	0.863	0.867	1.883	0.934	0.797	0.462	0.620	3.715	0.678	0.533	0.127	0.158
MGMN	2.730	0.829	0.683	0.495	0.561	0.358	0.991	0.963	0.975	0.975	0.544	0.884	0.817	0.871	0.869	4.476	0.822	0.689	0.351	0.450	4.143	0.579	0.445	0.107	0.115
Ours	1.037	0.925	0.795	0.701	0.751	0.044	0.994	0.960	0.994	0.997	0.299	0.904	0.839	0.901	0.903	0.993	0.962	0.850	0.601	0.717	3.568	0.701	0.549	0.177	0.195
Gain	19.9 %	1.8 %	3.0 %	11.4 %	6.4 %	48.8 %	0.0 %	-0.6 %	0.4 %	0.7 %	29.1 %	-1.5 %	0.0 %	2.4 %	1.6 %	31.6 %	0.6 %	1.8 %	5.4 %	5.1 %	2.2 %	1.2 %	1.9 %	18.0 %	12.1 %

Table 3: Experimental results of GSC. The bold represents the best performance. Gain is the percentage improvement of our model compared to the second place, and it is bolded to represent that our model improves performance on this metric. The experimental results show that our model achieves the best performance on 23 out of 25 metrics in five benchmark datasets compared to the state-of-the-art GSC method, which demonstrates the efficiency of our method.

best specifically on NCI109. *Based on these results, we select to use GCA for our model architecture on all datasets except NCI109, where we use sum pooling.*

The Impact of GNN Type, Enhancement of GIN, and Temperature Factor t . Here, we evaluate the impact of using different types of GNNs, whether to use Residual Connections and FFN to enhance GIN layers, and the temperature factor t of DiffAtt. The experimental results are shown in Table 2. Compared with GCN and GAT, GIN has a better overall performance due to its theoretically stronger expressiveness. Residual Connections can help to improve the training process, while FFNs could enhance the embedding of nodes, thus augmenting GIN leads to a stable and huge enhancement effect. Compared to using fixed temperature factors, learnable temperature factors can give better results for most metrics. Based on these results, our final model uses a GIN encoder with Residual Connections and FFNs, along with a DiffAtt module with learnable t , which can reach the best performance in most cases.

5.2 Main Results

We compare our REDRAFT with a number of state-of-the-art GSC methods: GMN (Li et al. 2019), SimGNN (Bai et al. 2019a), MGMN (Ling et al. 2021), GraphSim (Bai et al. 2020), EGSC (Qin et al. 2021) and ERIC (Zhuo and Tan 2022). We reimplemented all baseline models based on the hyperparameters provided in the original paper. For hyperparameters that were not provided, several experiments were conducted to find the optimal parameter values.

Table 3 presents the results of each model for a total of 25 metrics on the five benchmark datasets. **Overall, our model achieves state-of-the-art performance on 23 of the 25 metrics.** Especially on MSE, our model outperforms the second place by 19.9%, 48.8%, 29.1%, 31.6%, and 2.2%, respectively. Compared to GMN, GraphSim and MGMN with complex node interaction modules, REDRAFT achieves better performance with simple graph-level fusion modules, which illustrates the strong potential of graph-level embedding. Compared with other models using graph-level fusion modules, ERIC (NTN), SimGNN (NTN), and EGSC (EFN), REDRAFT uses DiffAtt to enhance the difference information in the graph-level embedding, thus making the representation of the graph-level embedding more flexible and representative, and substantially improving the performance of the model. This proves the high performance of the REDRAFT. Table 4 compares the training time, GPU mem-

	PTC			NCI109		
	Train(s)	Mem(MiB)	Infer(s)	Train(s)	Mem(MiB)	Infer(s)
GMN	259 ± 1.41	1375	2.6 ± 0.39	22646 ± 332.34	1425	259.2 ± 1.43
GraphSim	1868 ± 9.19	9142	5.9 ± 1.09	76231 ± 348.60	9212	661.2 ± 2.29
MGMN	1614 ± 1.41	16028	3.2 ± 0.43	59858 ± 485.08	13218	304.5 ± 2.94
REDRAFT	299 ± 3.54	1235	2.5 ± 0.43	20210 ± 225.57	1293	235.1 ± 0.86

Table 4: Experimental results of computational efficiency comparison between REDRAFT and node-level fusion models on larger graph datasets.

ory usage during training, and inference time of our graph-level fusion model REDRAFT against other node-level fusion models on two datasets that have the largest number of nodes in the available datasets, PTC (25.6 nodes on average) and NCI109 (28.9 nodes on average). The node-level fusion models like GraphSim and MGMN have considerably higher training times and GPU memory consumption compared to REDRAFT. In contrast, our REDRAFT is more efficient, reducing training time by 3.7 times and using 6.2 times lower GPU memory across the datasets on average. Moreover, REDRAFT has an advantage in inference speed. This efficiency advantage allows our method to scale to large-scale graphs.

6 RESAT: Quantifying Graph Fusion Modules' Ability

In this section, we propose a method called **Remaining Subgraph Alignment Test (RESAT)** to quantify the ability of different graph fusion modules in capturing graph structural difference information. Given graph pair G_i and G_j and a trained REDRAFT, *the core idea is to construct the graph structural difference between G_i and G_j into a single, valid graph $\bar{G}_{i,j}$. Then, by testing the similarity between the fused embedding $F(E(G_i), E(G_j))$ and the graph structural difference embedding $E(\bar{G}_{i,j})$, we can quantify how well the fusion module F captures the graph structural difference information to encode into the fused embedding.*

Data Processing. In order to construct graph structural difference into a single valid graph structure, for each graph G_i in the test set of the benchmark dataset, we construct subgraphs $G_{i,j}$ of it by sampling node subsets through random walks of length $\frac{N_i}{2}$ and including all edges between the sampled nodes. The proof provided in the appendix demonstrates that the mapping obtained when extracting subgraph $G_{i,j}$ from G_i is the optimal mapping between them. As

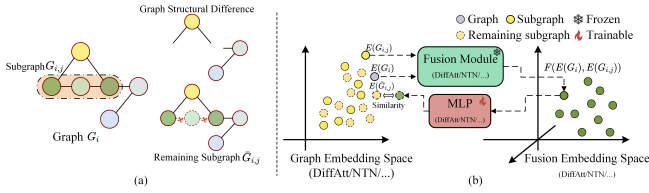


Figure 3: A diagram of the RESAT. (a) RESAT constructs the graph structural difference of G_i and its subgraph $G_{i,j}$ into a remaining subgraph $\bar{G}_{i,j}$. (b) Based on the different trained GNN Encoder E and fusion modules F , RESAT leverages an MLP to test the maximum similarity between the fused embedding $F(E(G_i), E(G_{i,j}))$ and the graph structural difference embedding $E(\bar{G}_{i,j})$.

shown in Fig 3(a), the *remaining subgraph* $\bar{G}_{i,j}$ is constructed by deleting all edges of $G_{i,j}$ in G_i and then deleting all isolated nodes, which maximally contains the graph structural difference between G_i and $G_{i,j}$ in a single valid graph, and is therefore well suited to be used as a graph representing the graph structural difference between G_i and $G_{i,j}$. In total, we construct 50 such $(G_{i,j}, \bar{G}_{i,j})$ pairs per graph G_i .

Methodology. We first train variants of REDRAFT on the benchmark datasets, replacing the fusion module F with different graph-level modules like NTN, EFN, etc. After training, the parameters of each encoder E and fusion module F are fixed. However, the original fusion embeddings and graph structural difference embeddings have different dimensions. Therefore, as shown in Fig 3(b), we train a new MLP regression model to map the embedding $F(E(G_i), E(G_{i,j}))$ to the target $E(\bar{G}_{i,j})$ to find their maximum similarity. For each fusion module F , the architecture of the MLP is adapted to optimize the mapping performance. The MSE loss between the fused graph embedding and the graph structural difference embedding reflects their optimal similarity. A lower MSE suggests the fused embedding has already encoded abundant graph structural difference features. This facilitates mapping it to the graph structural difference embeddings, implying the fusion module effectively captures graph structural difference. Conversely, a higher MSE indicates the fused embedding insufficiently represents graph structural difference. Hence it is harder to align with the graph structural difference embedding.

Results. The experimental results are shown in Table 5. We also report results for RESAT without any fusion module (No Fusion) and for graph-level fusion embedding before and after being adjusted by DiffAtt. Both NTN and No Fusion have poorer RESAT performance in most scenarios. However, NTN has lower accuracy in GSC because NTN focuses on the similarity of the two embeddings rather than the differences. Compared to No Fusion, EFN learns to capture graph structural difference information during the learning process without strong guidance from the internal architecture. Absolute distance performs better than squared distance (on average 1.365 vs 1.483 on GSC; on average 0.322 vs 1.424 on RESAT), probably because absolute distances better preserve the original distance information, whereas

	AIDS700nef		LINUX		IMDBMulti	
	GSC	RESAT	GSC	RESAT	GSC	RESAT
NTN	3.131	2.009	0.602	1.989	0.436	2.611
No Fusion	1.427	2.879	0.122	2.248	0.387	2.092
Square	1.497	0.313	0.062	0.289	0.442	0.386
EFN	1.346	1.024	0.070	0.950	0.392	0.901
Absolute	1.344	0.204	0.070	0.155	0.365	0.750
Before DiffAtt	1.096	1.008	0.062	0.644	0.316	1.179
After DiffAtt	0.099	0.105	0.105	0.105	0.116	0.116

	PTC		NCI109		ON AVERAGE	
	GSC	RESAT	GSC	RESAT	GSC	RESAT
NTN	5.965	6.443	3.648	0.383	2.756	2.687
No Fusion	1.539	2.057	3.650	3.276	1.425	2.510
Square	1.936	5.562	3.478	0.569	1.483	1.424
EFN	1.588	0.385	3.728	0.504	1.425	0.753
Absolute	1.558	0.189	3.488	0.310	1.365	0.322
Before DiffAtt	1.040	1.878	3.587	0.366	1.220	1.015
After DiffAtt	0.181	0.029	0.029	0.029	0.116	0.116

Table 5: Results of RESAT for various graph-level fusion modules, with the best result in bold. We also report the MSE accuracy of the model’s graph similarity calculation (GSC). *ON AVERAGE* denotes the average performance of each module on the five benchmark datasets.

squared distances reduce the impact of smaller differences. It is found that the adjusted graph fusion embedding with DiffAtt achieved a substantial improvement of 88.6% on average on RESAT compared to before the adjustment (0.116 vs 1.015), suggesting that DiffAtt substantially enhance the information from graph structural difference. We also find that the accuracy of GSC is closely correlated with the performance of RESAT, with a ρ of 0.899. This validates our hypothesis in Sec 3 that better capturing graph structural difference is key to modeling GED. DiffAtt outperforms the rest of the graph fusion modules on both GSC and RESAT, confirming that DiffAtt can better access the information from graph structural difference and thus better improve the performance of the model.

7 Conclusions and Limitations

This paper presents a novel graph-level fusion module, **DiffAtt**, inspired by the observation that the value of GED is only related to the graph structural difference between two graphs after optimal alignment. Based on DiffAtt, a new GSC model, **REDRAFT**, is proposed to achieve state-of-the-art performance in the GSC task. DiffAtt uses the difference between the two embeddings to enhance the information of graph structural difference in the graph-level embedding as attention, which substantially improves the performance of the model. Moreover, REDRAFT uses Residual Connections and FFNs to augment powerful expressive GINs to generate better graph-level embeddings. Compared with other state-of-the-art GSC models, REDRAFT achieves the best performance in 23 out of 25 metrics on five benchmark datasets. This paper also presents RESAT to quantify the ability of various graph-level fusion modules in capturing the graph structural difference, and the results show that DiffAtt can better capture graph structural difference information than other graph-level fusion methods.

There are several limitations to our work, the first being that REDRAFT as a GED predictor is not guaranteed to meet all properties of GED like triangular inequality and symmetry. Secondly, the additional use of FFNs in RE-

DRAFT reduces the speed of the model. Therefore, we encourage future work to address these issues and to better explore the potential of graph-level fusion.

References

- Ba, J. L.; Kiros, J. R.; and Hinton, G. E. 2016. Layer normalization. *arXiv preprint arXiv:1607.06450*.
- Bai, J.; and Zhao, P. 2021. TaGSim: type-aware graph similarity learning and computation. *Proceedings of the VLDB Endowment*, 15(2): 335–347.
- Bai, Y.; Ding, H.; Bian, S.; Chen, T.; Sun, Y.; and Wang, W. 2019a. Simgnn: A neural network approach to fast graph similarity computation. In *Proceedings of the Twelfth ACM International Conference on Web Search and Data Mining*, 384–392.
- Bai, Y.; Ding, H.; Gu, K.; Sun, Y.; and Wang, W. 2020. Learning-based efficient graph similarity computation via multi-scale convolutional set matching. In *Proceedings of the AAAI Conference on Artificial Intelligence*, volume 34, 3219–3226.
- Bai, Y.; Ding, H.; Qiao, Y.; Marinovic, A.; Gu, K.; Chen, T.; Sun, Y.; and Wang, W. 2019b. Unsupervised inductive graph-level representation learning via graph-graph proximity. *arXiv preprint arXiv:1904.01098*.
- Bougleux, S.; Brun, L.; Carletti, V.; Foggia, P.; Gaüzere, B.; and Vento, M. 2015. A quadratic assignment formulation of the graph edit distance. *arXiv preprint arXiv:1512.07494*.
- Fey, M.; and Lenssen, J. E. 2019. Fast graph representation learning with PyTorch Geometric. *arXiv preprint arXiv:1903.02428*.
- Gao, X.; Xiao, B.; Tao, D.; and Li, X. 2010. A survey of graph edit distance. *Pattern Analysis and applications*, 13(1): 113–129.
- He, K.; Zhang, X.; Ren, S.; and Sun, J. 2016. Deep residual learning for image recognition. In *Proceedings of the IEEE conference on computer vision and pattern recognition*, 770–778.
- Kendall, M. G. 1938. A new measure of rank correlation. *Biometrika*, 30(1/2): 81–93.
- Kipf, T. N.; and Welling, M. 2016. Semi-supervised classification with graph convolutional networks. *arXiv preprint arXiv:1609.02907*.
- Li, Y.; Gu, C.; Dullien, T.; Vinyals, O.; and Kohli, P. 2019. Graph matching networks for learning the similarity of graph structured objects. In *International conference on machine learning*, 3835–3845. PMLR.
- Liang, Y.; and Zhao, P. 2017. Similarity search in graph databases: A multi-layered indexing approach. In *2017 IEEE 33rd International Conference on Data Engineering (ICDE)*, 783–794. IEEE.
- Ling, X.; Wu, L.; Wang, S.; Ma, T.; Xu, F.; Liu, A. X.; Wu, C.; and Ji, S. 2021. Multilevel Graph Matching Networks for Deep Graph Similarity Learning. *IEEE Transactions on Neural Networks and Learning Systems*.
- Neuhaus, M.; Riesen, K.; and Bunke, H. 2006. Fast sub-optimal algorithms for the computation of graph edit distance. In *Joint IAPR International Workshops on Statistical Techniques in Pattern Recognition (SPR) and Structural and Syntactic Pattern Recognition (SSPR)*, 163–172. Springer.
- Qin, C.; Zhao, H.; Wang, L.; Wang, H.; Zhang, Y.; and Fu, Y. 2021. Slow Learning and Fast Inference: Efficient Graph Similarity Computation via Knowledge Distillation. *Advances in Neural Information Processing Systems*, 34.
- Ranjan, R.; Grover, S.; Medya, S.; Chakaravarthy, V.; Sabharwal, Y.; and Ranu, S. 2022. GREED: A Neural Framework for Learning Graph Distance Functions. In Oh, A. H.; Agarwal, A.; Belgrave, D.; and Cho, K., eds., *Advances in Neural Information Processing Systems*.
- Shrivastava, A.; and Li, P. 2014. A new space for comparing graphs. In *2014 IEEE/ACM International Conference on Advances in Social Networks Analysis and Mining (ASONAM 2014)*, 62–71. IEEE.
- Socher, R.; Chen, D.; Manning, C. D.; and Ng, A. 2013. Reasoning with neural tensor networks for knowledge base completion. *Advances in neural information processing systems*, 26.
- Spearman, C. 1961. The proof and measurement of association between two things.
- Tian, Y.; Mceachin, R. C.; Santos, C.; States, D. J.; and Patel, J. M. 2007. SAGA: a subgraph matching tool for biological graphs. *Bioinformatics*, 23(2): 232–239.
- Wale, N.; Watson, I. A.; and Karypis, G. 2008. Comparison of descriptor spaces for chemical compound retrieval and classification. *Knowledge and Information Systems*, 14: 347–375.
- Wang, L.; Zong, B.; Ma, Q.; Cheng, W.; Ni, J.; Yu, W.; Liu, Y.; Song, D.; Chen, H.; and Fu, Y. 2020. Inductive and unsupervised representation learning on graph structured objects. In *International conference on learning representations*.
- Wang, R.; Zhang, T.; Yu, T.; Yan, J.; and Yang, X. 2021. Combinatorial learning of graph edit distance via dynamic embedding. In *Proceedings of the IEEE/CVF Conference on Computer Vision and Pattern Recognition*, 5241–5250.
- Wang, X.; Ding, X.; Tung, A. K.; Ying, S.; and Jin, H. 2012. An efficient graph indexing method. In *2012 IEEE 28th International Conference on Data Engineering*, 210–221. IEEE.
- Xu, K.; Hu, W.; Leskovec, J.; and Jegelka, S. 2018. How powerful are graph neural networks? *arXiv preprint arXiv:1810.00826*.
- Yanardag, P.; and Vishwanathan, S. 2015. Deep graph kernels. In *Proceedings of the 21th ACM SIGKDD international conference on knowledge discovery and data mining*, 1365–1374.
- Zeng, Z.; Tung, A. K.; Wang, J.; Feng, J.; and Zhou, L. 2009. Comparing stars: On approximating graph edit distance. *Proceedings of the VLDB Endowment*, 2(1): 25–36.
- Zhang, Z.; Bu, J.; Ester, M.; Li, Z.; Yao, C.; Yu, Z.; and Wang, C. 2021. H2MN: Graph Similarity Learning with Hierarchical Hypergraph Matching Networks. In *Proceedings*

of the 27th ACM SIGKDD Conference on Knowledge Discovery & Data Mining, 2274–2284.

Zhuo, W.; and Tan, G. 2022. Efficient Graph Similarity Computation with Alignment Regularization. *Advances in Neural Information Processing Systems*, 35: 30181–30193.